

# Non-LTE LINE FORMATION FOR Zr I/II IN COOL STARS

A.B. Vinogradova, L.I. Mashonkina

Institut of Astronomy of Russian Academy of Sciences  
48 Pyatnitskaya st., Moscow 119017 Russia, *anna@inasan.ru*

**ABSTRACT.** Non-local thermodynamical equilibrium (non-LTE) line formation for neutral and singly-ionized zirconium is considered for the first time through a range of stellar parameters when the Zr abundance varies from the solar value down to  $[Zr/H] = -3$ . The model atom includes 63 combined energy levels of Zr I, 247 levels of Zr II and the ground state of Zr III. It is shown that the Zr I levels are depopulated relative to their thermodynamic equilibrium populations in the line formation layers with  $\log\tau_{5000} < 0.1$  resulting in weakening the Zr I lines relative to their LTE strengths. The ground state and low-excitation levels of Zr II keep their LTE populations throughout the atmosphere, while the excited levels of Zr II are overpopulated. This leads to weakening the Zr II lines arising from the ground state or low-excited levels. The role of inelastic collisions with hydrogen atoms in the statistical equilibrium of Zr I/II is estimated empirically from inspection of their different influences on Zr I and Zr II lines in the solar spectrum. The mean non-LTE abundance of zirconium in the solar atmosphere is determined as  $\log\epsilon_{Zr,\odot} = 2.61 \pm 0.09$  from the lines of two ionization stages, Zr I and Zr II. The dependence of non-LTE effects on the atmospheric parameters is considered for a small grid of model atmospheres with  $T_{eff} = 5500K$ ,  $\log g = 2.0$  and  $4.0$ ,  $[M/H] = -3.0, -2.0, -1.0,$  and  $0.0$ . The departures from LTE increase with increasing the luminosity and decreasing metal abundance (metallicity).

**Key words:** Line: formation; Sun: atmosphere; stars: abundance; line: profiles

## 1. Introduction

One believes that elements beyond the iron group are produced by neutron-capture reactions which are distinguished into slow (s-) and rapid (r-) process depending on the neutron density flux available. In ones turn, the slow process is subdivided into the main and the weak components. The weak s-process can run in the cores of massive ( $M \geq 20 M_{\odot}$ ) stars during hydrostatic helium-core burning, and the main s-process

occurs in intermediate-mass ( $2 - 4 M_{\odot}$ ), asymptotic-giant-branch (AGB) stars during unstable burning in the double shell source. According to Käppeler et al. [10], the weak s-process produces nuclei with an atomic mass  $A \leq 90$ . The r-process is associated with type II supernovae (SNeII). The different zirconium isotopes ( $A=90, 91, 92, 94, 96$ ) can be produced by various types of n-capture reactions. The current nucleosynthesis models are unable to predict the yields of elements in the r-process and give only very approximate estimates for the weak s-process. Therefore, one needs to reconstruct the history of the heavy-element enrichment of the interstellar medium on an observational basis and to provide accurate observational constraints to nucleosynthesis models.

In our recent work [17], the zirconium abundance was determined at the assumption of local thermodynamical equilibrium (LTE) in the atmospheres of 52 stars belonging to the Galactic thin disk, thick disk and halo. In the halo stars, a large overabundance of zirconium relative to barium is found up to  $\log(Zr/Ba) = 1.8$  at  $[Ba/H] = -3.8$  (Figure 1). The Zr/Ba ratio

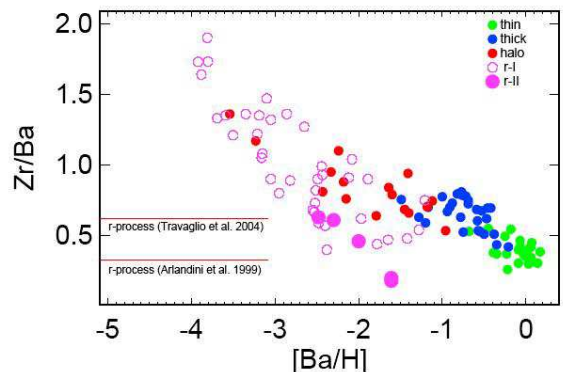


Figure 1:  $\log(Zr/Ba)$  abundance ratios as a function of  $[Ba/H]$  plotted based on the data from [4] and [17].

decreases with increasing the barium abundance and approaches to solar value in the thin disk stars. According to the current conceptions, the heavy elements in the early Galaxy were synthesized by pure r-process. Travaglio et al. [21] and Arlandini et al. [2] predict that the  $[Zr/Ba]$  ratio must be constant at  $[Fe/H] < -1.5$ . The observed trend points to the existence in the early

Galaxy of some additional source of synthesis of zirconium with only little contribution to barium.

The aim of this work is to check whether the departures from LTE can affect the observational finding on an evolutionary behavior of the stellar zirconium abundances.

## 2. The model atom

*Energy levels.* In the atmospheres of cool stars with  $T_{\text{eff}} = 5500 - 6500$  K, the major fraction of zirconium is represented by Zr II and a fraction of Zr I does not exceed several parts in a thousand. Zr II is a species of our main interest because only Zr II lines are observed in metal-poor stars. We use all measured energy levels of Zr II with an excitation energy up to  $E_{\text{exc}} = 8.75$  eV available in the NIST (<http://physics.nist.gov/PhysRefData>) database and in Malcheva et al. [16]. However, an ionization energy of Zr II is 13.13 eV, and we use the predicted high-excitation levels from calculations of H. Nilsson [18] in order to provide close coupling to the next ionization stage. The model atom of Zr I includes the measured levels from the NIST and VALD (Kupka et al. [11]) databases with  $E_{\text{exc}}$  up to 4.25 eV. In total, the model atom is based on 148 levels of Zr I and 772 levels of Zr II. The levels with small energy differences were combined into single level. The resulting model atom consists of 63 levels of Zr I, 247 levels of Zr II, and the ground state of Zr III. Fine structure is allowed for low excited levels of Zr II with  $E_{\text{exc}} < 5$  eV.

*Radiative bound-bound (b-b) rates.* For Zr II, we take into account 1070 experimental oscillator strengths from [14] and 8266 theoretical ones from [18]. For Zr I, we use only experimental oscillator strengths taken from the NIST and VALD databases for 247 transitions.

*Photoionization cross-sections.* We apply hydrogenic approximation because no accurate data is available.

*Collisional rates.* The electron impact excitation is taken into account using the van Regemorter's formula [22] for the allowed transitions and using a line collision strength,  $\Omega_{ij} = 1$  for the forbidden transitions. The electron impact ionization is calculated using the Drawin's formula [8]. In the atmospheres of cool stars, a number of neutral hydrogen atoms is much larger than a number of electrons. Therefore, one also needs to take into account collisions with hydrogen atoms. We use the Steenbock & Holweger's formula [19] for allowed transitions and Takeda's approximation [20] for forbidden transitions. Since both formulas provide only an order of magnitude accuracy, we made test calculations varying a scaling factor to these formulas,  $k_{\text{H}}$ , between 0 and 1 to determine it empirically.

## 3. Methods and codes

In our calculations, we use plane-parallel, homogeneous, blanketed model atmospheres computed using the MAFAGS code [9]. We set an  $\alpha$ -element enhancement  $[\alpha/\text{Fe}] = 0$  for the models with  $[\text{M}/\text{H}] > -0.6$  and  $[\alpha/\text{Fe}] = 0.4$  for the less metallicity models. We use a revised version of the DETAIL program [7] based on the accelerated  $\Lambda$ -iteration in order to solve the coupled radiative transfer and statistical equilibrium equations. The departure coefficients obtained from DETAIL are then applied to compute synthetic line profiles via the SIU program developed by T. Gehren and J. Reetz at the University of Munich. The list of spectral lines includes all atomic and molecular lines from tables of Kurucz [13].

## 4. Mechanisms of departure from LTE

Figure 2 shows the departure coefficients,

$$b_i = \frac{n_i}{n_i^*}$$

of the selected levels of Zr I and Zr II as a function of continuum optical depth  $\tau_{5000}$  at  $\lambda = 5000\text{\AA}$  in the solar atmosphere. Here,  $n_i$  and  $n_i^*$  are the statistical equilibrium and LTE (Saha-Boltzmann) number densities, respectively. We find that the ground state and low-excitation levels of Zr II keep their LTE populations, but other levels of Zr II are overpopulated due to radiative pumping from the ground state and low excited levels. When hydrogenic collisions are neglected for forbidden transitions, a small depopulation of some low excited levels is seen at  $\log \tau_{5000} < -2$ . Opposite, most Zr I levels are depopulated everywhere above  $\log \tau_{5000} = 0$  due to ultraviolet overionization.

We find that for every Zr I and Zr II line used in the zirconium abundance analysis, the upper level is overpopulated relative to the lower level of the transition. In the visual spectral range, a line source function is

$$S_\nu \approx B_\nu \frac{b_j}{b_i},$$

where  $b_j$  and  $b_i$  are the departure coefficients of the upper and lower levels, respectively, and  $B_\nu$  is the Planck function. Since the upper level is overpopulated relative to the lower level,

$$\frac{b_j}{b_i} > 1$$

is valid, and, consequently,  $S_\nu > B_\nu$ . As a result, the line is weakened. Thus, in order to fit the observed profile of the line, one needs to increase an abundance of the zirconium. The non-LTE effects lead to positive

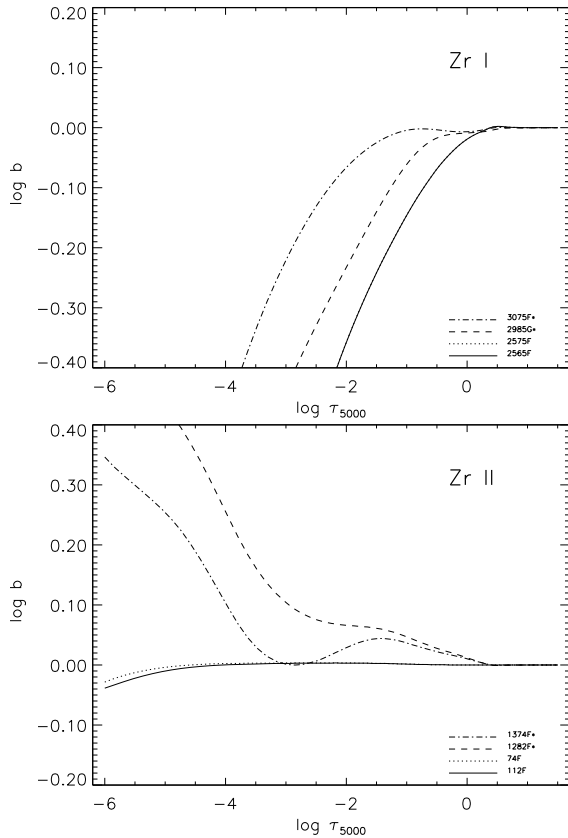


Figure 2: Departure coefficients of some Zr I/II levels as a function of  $\log \tau_{5000}$  in the solar atmosphere.

non-LTE abundance corrections.

## 5. Analysis of the Zr I and Zr II lines in the solar spectrum

### 5.1. The spectral line sample

The abundance of zirconium in the solar atmosphere was determined in several papers under the LTE assumption. Biémont et al [5] used the equivalent width method for 34 lines of Zr I and 24 lines of Zr II. They have obtained the mean abundances derived from the lines of two ionization stages to be consistent, but with large abundance errors of up to 0.21 dex.

Ljung et al. [14] use the equivalent widths for 7 most reliable lines of Zr II and determine the solar Zr abundance with the abundance error of 0.02 dex. Bogdanovich et al. [6] apply theoretical oscillator strengths and determine the solar Zr abundance from 21 lines of Zr I and 15 lines of Zr II. Having inspected the zirconium lines in the solar flux spectrum [12] we find that many of them are blended and the equivalent width method cannot provide correct calculations of the blending lines effect. We conclude that most lines from the Biémont's line list cannot be used

in abundance analysis. We find only 6 relatively unblended lines of Zr I and 10 lines of Zr II which can be reliably used to determine the zirconium abundance in the solar atmosphere.

### 5.2 The zirconium abundance in the solar atmosphere

We make calculations for a model atmosphere with  $T_{\text{eff}} = 5780$  K,  $\log g = 4.44$ , microturbulence velocity  $V_{\text{mic}} = 0.9 \text{ km s}^{-1}$ . Our synthetic flux profiles are convolved with a profile that combines a rotational broadening of  $1.8 \text{ km s}^{-1}$  and broadening by macroturbulence with a radial-tangential profile of  $V_{\text{mac}}$  which was allowed to vary between  $2.4 \text{ km s}^{-1}$  and  $4 \text{ km s}^{-1}$  for different lines. Figure 3 shows the best fits of the selected Zr I and Zr II lines achieved with the Zr abundance  $\log \varepsilon_{\text{Zr}} = 2.57$  dex for Zr I 4687 Å and 2.68 dex for Zr II 4208 Å.

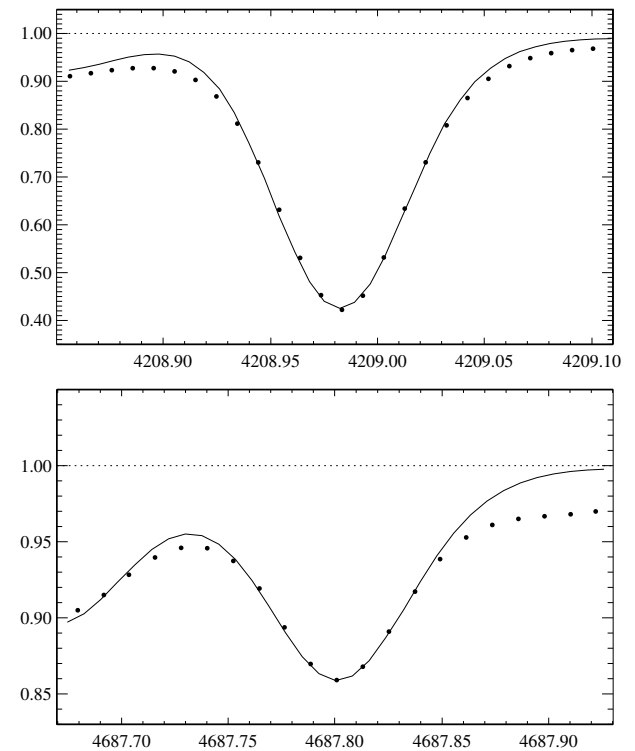


Figure 3: Best non-LTE fits of the solar Zr I 4687Å and Zr II 4208Å lines. See text for more details.

The largest uncertainty of our non-LTE calculations is connected with a treatment of hydrogenic collisions. According to various investigations, the Steenbock & Holweger's formula [19] overestimates  $C_{ij}(\text{H})$ . We determine a scaling factor,  $k_{\text{H}}$ , to this formula from analysis of the Zr I and Zr II lines in the solar spectrum. The test calculations are performed for 8 cases, namely, LTE, non-LTE neglecting hydrogen collisions, non-LTE including hydrogen collisions only for allowed

transitions with  $k_H = 0.1, 0.33, 1.0$ , and non-LTE including hydrogen collisions for both allowed and forbidden transitions with  $k_H = 0.1, 0.33, 1.0$ . For each case, we determine the average element abundances from the Zr I lines and from the Zr II lines. The results are presented in Figure 4. It is evident, every non-LTE case provides the smaller discrepancy between the element abundances from two ionization stages than the LTE case where the abundance difference is  $\log \varepsilon_{\text{ZrII}} - \log \varepsilon_{\text{ZrI}} = 0.27$ .

If hydrogen collisions are neglected, the non-LTE effects are maximal. We prefer the case when hydrogen collisions are taken into account for both allowed and forbidden transitions with  $k_H = 0.1$ . In this case, a well agreement is simultaneously achieved between the element abundances from two ionization stages,  $\log \varepsilon_{\text{ZrII}} - \log \varepsilon_{\text{ZrI}} = 0.04$ , as well as between the solar average Zr abundance ( $\log \varepsilon_{\text{Zr}} = 2.61 \pm 0.09$ ) and the meteoritic value ( $\log \varepsilon_{\text{Zr}} = 2.57$  [3], 2.60 [15] and 2.61 [1]). We use an usual abundance scale where  $\log \varepsilon_{\text{H}} = 12$  for hydrogen.

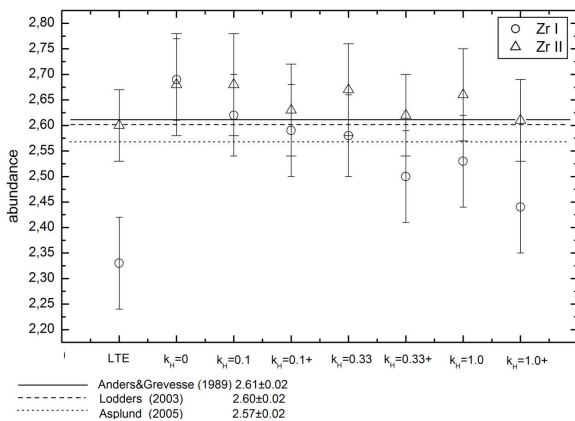


Figure 4: Mean abundances determined from the solar Zr I (circles) and Zr II (triangles) lines for various line formation treatments compared to the meteoritic Zr abundance from [1] (continuous line), [3] (dotted line), and [15] (dashed line). See text for more details.

## 6. Non-LTE effects as a function of stellar parameters

We calculate a non-LTE abundance correction,  $\Delta_{\text{NLTE}} = \varepsilon_{\text{NLTE}} - \varepsilon_{\text{LTE}}$ , for the Zr II lines for a small grid of model atmospheres with an effective temperature  $T_{\text{eff}} = 5500$  K,  $\log g = 2.0$  and  $4.0$ , and  $[M/H] = -3.0, -2.0, -1.0$ , and  $0.0$ . The results are shown in the Figure 5. It can be seen that the non-LTE effects are small for  $\log g = 4.0$ :  $\Delta_{\text{NLTE}}$  does not exceed 0.06 dex. For  $\log g = 2.0$ ,  $\Delta_{\text{NLTE}}$  depends strongly on metallicity and increases from 0 up to 0.6 dex with decreasing  $[M/H]$  from 0 to  $-2$ .

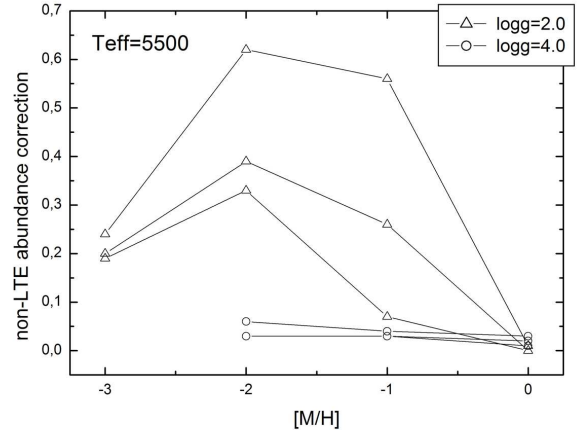


Figure 5: Non-LTE abundance corrections for lines of Zr II 3479, 3505, 4208 ÅÅ (the values at  $\log g = 2$ , triangles), and Zr II 3505, 3714, 4208 ÅÅ (the values at  $\log g = 4$ , circles) as a function of stellar parameters.

This is due to decreasing the electron number density and, hence, decreasing collisional rates. The non-LTE abundance corrections start to decrease with further decreasing  $[M/H]$  due to a shift of the line formation depth to deeper layers.

## 7. Conclusions

We have treated the model atom of Zr I/II including 63 combined levels of Zr I, 247 levels of Zr II and the ground state of Zr III. We show that the excited levels of Zr II are overpopulated relative to their LTE populations, while the Zr I levels are underpopulated. We deduce from analysis of the Zr I and Zr II lines in the solar spectrum that one needs to take into account hydrogenic collisions in SE calculations for both allowed and forbidden transitions with a scaling factor  $k_H = 0.1$  to the Steenbock & Holweger's formula. In this case, the absolute abundance of zirconium in the solar atmosphere amounts  $2.61 \pm 0.09$  dex. Test calculations for the grid of model atmospheres with  $T_{\text{eff}} = 5500$  K show that the non-LTE effects are small for dwarf stars with  $\log g = 4.0$ . In giants ( $\log g = 2.0$ ), the non-LTE abundance corrections depend strongly on metallicity and increase from 0 up to 0.6 dex with decreasing  $[M/H]$  from 0 to  $-2$ . They start to decrease with further decreasing  $[M/H]$ .

*Acknowledgements.* This research was supported by the the Russian Foundation for Basic Research with grant 08-02-00469-a and the Presidium RAS Programme "Origin and evolution of stars and the Galaxy".

## References

1. Anders E. & Grevesse N.: 1989, *Geoch. & Cosmochim Acta*, **53**, 197.
2. Arlandini C., Kappeler F., Wisshak K. et al.: 1999, *Astrophys. J.*, **525**, 886
3. Asplund M., Grevesse N. & Sauval A.J.: 2005 *ASP Conf. Ser.*, **336**, 25
4. Barklem P.S., Christlieb N., Beers T.C., et al.: 2005, *Astron. & Astrophys.*, **439**, 129
5. Biémont E. & Grevesse N.: 1981, *Astrophys. J.*, **248**, 867
6. Bogdanovich P., Tautvaisiene G., Rudzikas Z., Momkauskaite A.: 1996, *MNRAS*, **280**, 95
7. Butler K. & Giddings J.: 1985, *Newsletter on the analysis of astronomical spectra 9*, University of London
8. Drawin H. W.: 1961, *Z. Phys.*, **164**, 513
9. Fuhrmann K., Pfeiffer M., Frank C., et al.: 1997, *Astron. & Astrophys.*, **323**, 909
10. Käppeler F., Beer H., & Wisshak K.: 1989, *Rep. Prog. Phys.*, **52**, 954
11. Kupka F., Piskunov N., Ryabchikova T.A., et al.: 1999, *Astron. & Astrophys.*, **138**, 119
12. Kurucz R. L., Furenlid I., Brault J., & Testerman, L.: 1984, *NSO Atlas No. 1: Solar Flux Atlas from 296 to 1300 nm, Sunspot, NSO*
13. Kurucz R.L.: 1994 *CD-Roms No. 18, 19*
14. Ljung G., Nilsson H., Asplund M., & Johansson S.: 2006, *Astron. & Astrophys.*, **456**, 1181
15. Lodders K.: 2003, *Astrophys. J.*, **591**, 1220
16. Malcheva G., Blagoev K., Mayo R., et al.: 2006, *MNRAS*, **367**, 754
17. Mashonkina L.I., Vinogradova A.B., Ptitsyn D.A. et al.: 2007, *Astronomy Reports*, **51**, 11
18. Nilsson H.: 2007 (private communication)
19. Steenbock W. & Holweger H.: 1984, *Astron. Astrophys.*, **130**, 319
20. Takeda Y.: 1994, *PASJ*, **46**, 53
21. Travaglio C., Galli D., Gallino R., et al.: 1999, *Astrophys. J.*, **521**, 691
22. van Regemorter H.: 1962, *Astrophys. J.*, **136**, 906